

## Catalog of Multi–Mode Radially Pulsating Variables: I

A. V. Khruslov<sup>1,2</sup>

<sup>1</sup> Sternberg Astronomical Institute, Moscow State University, Universitetskij pr. 13, Moscow 119992, Russia; khruslov@bk.ru

<sup>2</sup> Institute of Astronomy, Russian Academy of Sciences, Pyatnitskaya str. 48, Moscow 119017, Russia

I present a catalog of newly detected Multi-Mode Radially Pulsating (MMRP) variable stars that pulsate in the fundamental, first, second, or third-overtone modes. This catalog includes 50 double- and multi-mode stars. Among variability types of these stars, we find classical Cepheids, RR Lyrae, and high-amplitude  $\delta$  Scuti (HADS) variables. Additionally, I studied 14 known multi-periodic variables.

I analyzed all observations available for these stars in the ASAS-SN and ZTF online public archives using the period-search software developed by Dr. V.P. Goranskij for Windows environment. Light elements and parameters of oscillations were determined.

## 1 Introduction

In the course of my search for double-mode and multiperiodic variable stars using available photometric archives, I detected 50 new Multi-Mode Radially Pulsating (MMRP) variables. These stars pulsate in the fundamental, first-overtone, second-overtone, or third-overtone modes. This article continued the series of my previous papers (Khruslov. 2018a, 2021a, 2022, etc.). Among variability types of these stars, we find classical Cepheids, RR Lyrae stars, and high-amplitude  $\delta$  Scuti variables.

Additionally, I studied 14 known multi-periodic variables (see additional Tables with index 'a') as a part of the program of preparation for their inclusion in the General Catalog of Variable Stars, GCVS (Samus et al., 2017).

Searching for double periodicity, I mainly used data available in the photometric archive of the All-Sky Automated Survey for Supernovae (ASAS-SN, Shappee et al., 2014; Kochanek et al., 2017) and the Zwicky Transient Facility (ZTF, Bellm et al., 2019; Masci et al., 2019)

The method I use to search for multiperiodicity is similar to that described in my earlier paper (Khruslov, 2021). To search for candidate multi-mode variables, I used AAVSO VSX<sup>1</sup> database, the ASAS-SN catalogs of variable stars<sup>2</sup> database (Jayasinghe et al., 2018, 2019a, 2019b, 2020, 2021), ZTF catalog of periodic variable stars<sup>3</sup>, Chen et al. (2020).

The radial pulsation modes were identified by their period ratio ( $P_{\text{short}}/P_{\text{long}}$ ); see the study on this problem by Petersen (1973), Petersen & Christensen-Dalsgaard (1996), Smolec & Moskalik (2010), and others.

<sup>1</sup> <http://www.aavso.org/vsx/index.php?view=search.top>

<sup>2</sup> <https://asas-sn.osu.edu/variables>

<sup>3</sup> <http://variables.cn:88/ztf/>

## 2 Photometric data

For this study, I used the data of the ASAS-SN<sup>4</sup> database and the ZTF data available through the SNAD ZTF viewer<sup>5</sup>, Malanchev et al. (2021). The light elements are based on data from these two surveys, individual cases are described in Comments. The magnitude ranges and amplitudes in the tables are given according to this data. I used  $V$  and  $g$  bands of ASAS-SN, and  $r$  and  $g$  bands of ZTF.

Additionally, in individual cases, I analyzed available data from other archives: the Wide Angle Search for Planets (SuperWASP<sup>6</sup>, Butters et al., 2010; 8 variables), the Catalina Sky Surveys (CSS<sup>7</sup>, Drake et al., 2009; 5 variable), the All Sky Automated Survey (ASAS-3<sup>8</sup>, Pojmanski 2002; 2 variables).

The ASAS-3 data used in this paper were downloaded before April 2022, in accordance to requirements of authors of this survey for users located in Russia.

The SuperWASP observations are available as FITS tables, which were converted into ASCII tables using the OMC2ASCII<sup>9</sup> program, as described by Sokolovsky (2007).

The survey data used in this study for the program stars are available online in the html version of this paper as a zip archive. This file also includes all light curves of the variables and cross-identification tables for all stars.

In individual cases, the ZTF data contained continuous data series with duration of a whole night of observations. This created some difficulties in the analysis of data. To eliminate these problems, we used averaged values (the mean for about 10 neighboring points) for our analysis. These averaged values are presented in the data files below the main data series. The rows of these supplements contain mean HJD times, mean magnitudes, and number of averaged points.

## 3 Identification names

In this paper, the following identification names are used for variables.

For new multi-periodic stars, with multi-periodicity first detected in this study, I use designations of the form MMRP–XXX (where MMRP is the name of the present program, aimed at discoveries of Multi-Mode Radially Pulsating variables, and XXX is the sequence number in the catalog). An example: MMRP–010.

For the known multi-periodic stars, for which this paper presents new light elements, I used designations in the form MMRP\_JXXXXXX.XX+XXXXXX.X (the abbreviation MMRP followed with equatorial coordinates for the equinox 2000.0). An example: MMRP\_J054223.13+275647.6.

## 4 Classification

In the present paper, I use an original notation for types of multiperiodic variables. The basics of the classification were presented by N.N. Samus and the GCVS team at the XXVI IAU General Assembly in Prague, 2006<sup>10</sup>: classical GCVS types of radial pulsating variables were appended with numbers of pulsation modes (0 – fundamental mode, 1 –

<sup>4</sup> <https://asas-sn.osu.edu/>

<sup>5</sup> <https://ztf.snad.space/>

<sup>6</sup> <http://wasp.cerit-sc.cz/form/>

<sup>7</sup> [http://nunuku.caltech.edu/cgi-bin/getcssconedb\\_release.img.cgi](http://nunuku.caltech.edu/cgi-bin/getcssconedb_release.img.cgi)

<sup>8</sup> <http://www.astrouw.edu.pl/asas/?page=aasc>

<sup>9</sup> [http://scan.sai.msu.ru/swasp\\_converter/](http://scan.sai.msu.ru/swasp_converter/)

<sup>10</sup> <http://www.sai.msu.su/gcvs/future/classif.htm>

first overtone, 2 – second overtone). Double-mode variables are marked with a set of detected modes. For example, RR Lyrae stars can be designated as RR0, RR1, and RRB01 (in the old system, RRAB, RRC, and RR(B), respectively, B meaning “beat”). A similar notation was proposed for classical Cepheids (DCep0, DCep1, DCepB01, and DCepB12).

In the new MMRP classification, the numerical identification of pulsation modes is preserved, and the variability type is designated with a single letter. Additional characteristics are introduced with an additional index. An arrow indicates the cases of mode switching.

### I. Types of variable stars:

- C – classical Cepheids;
- W – W Virginis, or type II Cepheids;
- R – RR Lyrae stars;
- D –  $\delta$  Scuti stars.

### II. Numbers of pulsation modes:

- 0 – fundamental mode;
- 1 – first overtone;
- 2 – second overtone;
- 3 – third overtone.

### III. Addition designations:

- n – additional non-radial mode;
- m – amplitude modulation;
- $\rightarrow$  – mode switching.

Examples of designations of multi-periodic variables: C01, C12, C12m, D01, D123, D23, D12n, D0123, R01, W01, C12 $\rightarrow$ C1, R01 $\rightarrow$ R0, R1 $\rightarrow$ R01.

The classical GCVS designations of mono-periodic variability types can be converted as follows: DCEP = C0, DCEPS = C1, RRAB = R0, RRC = R1; for multi-mode variable types, RR(b) type can be written as R01 (there are no R12 stars confirmed with certainty); CEP(B) is a group of types designated as C01, C12, C012, C123, and W01; DSCT(B) and SXPHE(B) is a group of all multi-mode D types.

The types from the VSX database are converted as follows: RRd = R01; DCEP(B) = C01; DCEPS(B) = C12; CWB(B) = W01; HADS(B) is a group of all multi-mode D types.

Double-mode type II Cepheids (W Virginis type) and mode-switching stars are not included in this catalog. An example of a W01 star, USNO-B1.0 0992-0344981, can be found in Khruslov (2021). An example of an R01 $\rightarrow$ R0 star is USNO-B1.0 1171-0309158, see Khruslov et al. (2017). Other stars of these types may be included in later issues of MMPR catalogs.

in addition to type C12, I used type C\*12 that includes stars morphologically close to type C12 but with shorter periods characteristic of R1 stars (see Subsection 6.3).

Besides the basic classification, I used two other indices: n for cases of detected additional non-radial modes; m for detected amplitude modulation with slow variation from

one season to another.

## 5 Results

### 5.1 Tables

For a correct presentation of information on multi-periodic variables in the MMRP catalog Tables, I use a multi-row format, with data presented in several sub-rows, each of them corresponding to an individual detected radial pulsation mode. Modes of pulsations are arranged in order of increasing pulsation frequency: the top sub-row is fundamental mode, the first overtone is below it, still lower are the second overtone, third overtone, and so on.

Each multi-row of the main Table (see Tables 1 and 1a) contains general information on the star: number in the Catalog of Multi-Mode Radially Pulsating (MMRS) stars; equatorial coordinates J2000 (for the earlier known MMRP stars, the coordinates are a part of the name); magnitude range (magnitudes at maximum and at minimum); type of multi-periodicity; and then, information about individual modes is presented in sub-rows (light elements, period and epoch of maximum; semi-amplitude; asymmetry parameter of the phased light curve, M–m). The period ratio (shorter period / longer period) is given for each pair of adjacent sub-rows (in the sub-row for the longer period).

The equatorial coordinates are given according to the Gaia EDR3 catalog. The tabulated magnitude range is for the photometric band indicated in brackets ( $aV$  and  $ag$  are ASAS-SN  $V$  and  $g$  magnitudes;  $zr$  and  $zg$  are ZTF  $r$  and  $g$  magnitudes). The data in these two columns are in two adjacent sub-rows. Coordinates: top – Right Ascension, bottom – Declination; magnitude range: top – maximum, bottom – minimum.

Individual mode characteristics: period is expressed in days; epoch is in one of the following formats:  $E = aX.XXXX = HJD - 2457777.0$  or  $E = bX.XXXX = HJD - 2458888.0$ ; semi-amplitude in the photometric band indicated in the “Magn.” column; the M–m parameter is expressed in fractions of the period.

Tables 2 and 2a contain references to comments that supplement the data in the main table, and also provide information about the history of the variability studies for individual stars. The numbers correspond to the list below the tables.

Tables that supplement the main Table (Table 1 with Comments) follow, they contain general information on the stars. Tables 3 and 3a contain semi-amplitudes and magnitude ranges in all bands used in the ASAS-SN and ZTF surveys:  $aV$ ,  $ag$ ,  $zr$ , and  $zg$ . The data in “Magnitude range” columns is separated between two adjacent sub-rows: top – maximum, bottom – minimum. These tables contain amplitudes for four bands, so they partially duplicate Tables 1 and 1a. Tables 4 and 4a contain the known information according to catalogs and photometric surveys: color indices  $J - K$  (2MASS),  $B - V$  and  $g' - r'$  (APASS),  $g - V$  (ASAS-SN), and  $g - r$  (ZTF); and Galactic latitude (in degrees). These data are used for classification of variables.

**Table 1. New MMRP variables**

MMRP	J2000	Magn.	Type	Period	Epoch	Ampl.	M–m	$P_S/P_L$
001	00 02 40.26 +62 48 07.1	17.12 – 17.63 ( <i>zg</i> )	D12m	0.221546 0.177851	b0.020 b0.150	0.159 0.060	0.40 0.50	0.8028
002	00 14 03.41 +61 51 26.8	15.40 – 15.94 ( <i>zg</i> )	D123	0.2402248 0.1917915 0.1599293	b0.2335 b0.1130 b0.0683	0.149 0.034 0.039	0.44 0.47 0.45	0.7984 0.8339
003	00 53 46.41 +16 30 17.6	17.73 – 18.47 ( <i>zg</i> )	R01	0.553765 0.413406	b0.060 b0.345	0.086 0.224	0.44 0.34	0.7465
004	01 04 59.14 +63 11 37.9	16.12 – 16.70 ( <i>zg</i> )	C12	0.517962 0.415517	b0.234 b0.282	0.230 0.018	0.50 0.48	0.8022
005	01 22 26.27 +59 12 36.2	12.26 – 12.68 ( <i>ag</i> )	C*12	0.419811 0.335806	b0.347 b0.069	0.140 0.035	0.50 0.46	0.7999
006	01 41 37.16 +49 06 30.3	17.66 – 18.41 ( <i>zg</i> )	R01	0.547006 0.408560	b0.148 b0.132	0.059 0.238	0.44 0.35	0.7469
007	02 35 16.88 +45 29 06.0	13.94 – 14.32 ( <i>zg</i> )	D12	0.1171010 0.0955676	a0.0560 a0.0013	0.118 0.036	0.38 0.46	0.8161
008	03 28 13.47 +61 04 11.4	15.16 – 15.58 ( <i>zr</i> )	C12	0.76234 0.61488	b0.703 b0.585	0.133 0.045	0.45 0.45	0.8066
009	04 50 39.61 +44 56 33.7	14.44 – 15.11 ( <i>zg</i> )	C12	0.481392 0.385787	a0.122 a0.128	0.257 0.043	0.49 0.48	0.8014
010	04 53 16.75 +39 14 18.2	14.37 – 15.21 ( <i>ag</i> )	D0123	0.323070 0.243812 0.195780 0.163560	b0.036 b0.100 b0.113 b0.147	0.164 0.136 0.025 0.023	0.37 0.55 0.43 0.50:	0.7547 0.8030 0.8354
011	05 55 38.69 +27 03 19.9	13.99 – 14.48 ( <i>zg</i> )	C*12	0.372014 0.298223	b0.039 b0.185	0.193 0.022	0.52 0.50	0.8016
012	06 32 45.23 –57 48 19.8	12.56 – 13.04 ( <i>aV</i> )	D012	0.1202966 0.0910362 0.0732255	a0.1160 a0.0660 a0.0314	0.005 0.187 0.013	0.47 0.36 0.45	0.7568 0.8044
013	06 35 07.25 –02 24 39.4	18.12 – 18.81 ( <i>zr</i> )	R01	0.485603 0.361474	b0.415 b0.370	0.127 0.155	0.44 0.38	0.7444
014	07 04 53.11 +72 56 03.8	16.53 – 17.61 ( <i>zg</i> )	D012	0.0990373 0.0774669 0.0625011	b0.0412 b0.0343 b0.0240	0.208 0.111 0.036	0.33 0.41 0.43	0.7822 0.8068

**Table 1 (continued)**

MMRP	J2000	Magn.	Type	Period	Epoch	Ampl.	M-m	$P_S/P_L$
015	07 17 06.72 +02 10 06.3	14.11 – 14.50 ( <i>zg</i> )	D12	0.1777760 0.1426887	b0.1080 b0.1100	0.128 0.032	0.45 0.48	0.8026
016	07 19 18.34 –57 21 50.8	14.01 – 14.50 ( <i>aV</i> )	D12m	0.09090585 0.07264440	a0.0800 a0.0595	0.164 0.032	0.41 0.45	0.7991
017	07 34 28.23 –09 23 48.5	16.36 – 17.09 ( <i>zg</i> )	R01	0.517177 0.385962	b0.253 b0.225	0.069 0.231	0.46 0.36	0.7463
018	07 41 56.58 –05 35 59.7	13.68 – 14.10 ( <i>ag</i> )	D12	0.1170699 0.0937507	a0.0088 a0.0044	0.141 0.027	0.48 0.46	0.8008
019	07 42 26.28 –48 26 25.9	12.66 – 12.90 ( <i>aV</i> )	D12m	0.1633818 0.1303208	b0.1555 b0.1240	0.080 0.007	0.54 0.48	0.7976
020	08 09 53.53 –24 00 01.5	12.66 – 13.16 ( <i>ag</i> )	D23	0.1894973 0.1569780	b0.063 b0.095	0.174 0.034	0.30 0.48	0.8284
021	09 20 33.29 –53 23 17.3	13.24 – 13.57 ( <i>ag</i> )	C12	0.962282 0.773766	b0.550 b0.567	0.100 0.026	0.44 0.50:	0.8041
022	10 14 19.37 –45 08 07.4	14.74 – 15.38 ( <i>ag</i> )	D01n	0.1849927 0.1413880	b0.0420 b0.0640	0.113 0.108	0.38 0.55	0.7643
023	10 17 57.49 –43 33 27.5	12.99 – 13.30 ( <i>ag</i> )	D12	0.1604404 0.1271510	b0.1380 b0.0520	0.106 0.013	0.53 0.46	0.7925
024	10 20 35.06 –45 27 09.0	13.50 – 14.03 ( <i>ag</i> )	D012m	0.1828460 0.1401066 0.1120996	b0.1275 b0.0290 b0.1050	0.103 0.105 0.011	0.40 0.59 0.50	0.7663 0.8001
025	11 00 35.99 –00 33 15.9	17.95 – 18.50 ( <i>zg</i> )	D01	0.0762403 0.0592999	b0.0522 b0.0572	0.134 0.057	0.39 0.49	0.7778
026	12 18 49.01 –40 36 23.7	13.73 - 14.11 ( <i>ag</i> )	D12	0.1206566 0.0965767	a0.0237 a0.0860	0.132 0.012	0.56 0.47	0.8004
027	14 00 12.79 –57 59 22.8	11.46 - 11.75 ( <i>ag</i> )	C*12	0.3422644 0.2735650	b0.886 b0.876	0.086 0.021	0.47 0.46	0.7993
028	15 23 19.83 –29 23 55.8	15.52 - 16.25 ( <i>ag</i> )	D01	0.06193270 0.04790184	b0.0094 b0.0090	0.184 0.044	0.40 0.48	0.7734
029	16 36 55.57 –29 40 06.6	14.12 - 14.50 ( <i>ag</i> )	D01	0.0961730 0.0742609	b0.0150 b0.0387	0.068 0.044	0.43 0.45	0.7722

**Table 1 (continued)**

ID	J2000	Magn.	Type	Period	Epoch	Ampl.	M-m	$P_S/P_L$
030	16 40 26.77 +02 17 42.7	14.76 - 15.34 ( <i>ag</i> )	D01	0.06017101 0.04669287	b0.0103 b0.0006	0.132 0.069	0.40 0.44	0.7760
031	17 22 56.98 -37 09 12.4	14.29 - 14.78 ( <i>ag</i> )	D23	0.1900259 0.1573530	a0.0420 a0.0870	0.143 0.032	0.44 0.46	0.8281
032	17 32 05.89 -29 55 58.7	13.15 - 13.48 ( <i>aV</i> )	D12m	0.2959543 0.2361465	a0.0820 a0.0824	0.103 0.022	0.56 0.45	0.7979
033	18 04 41.13 -28 56 05.0	11.49 - 12.12 ( <i>aV</i> )	D01m	0.1929179 0.1481671	a0.0292 a0.1310	0.199 0.056	0.37 0.47	0.7680
034	18 29 59.91 +11 23 01.2	13.85 - 14.25 ( <i>zg</i> )	D01	0.06896850 0.05332345	b0.1162 b0.0420	0.119 0.040	0.44 0.47	0.7732
035	18 39 23.75 -53 36 50.9	14.99 - 15.86 ( <i>ag</i> )	D01	0.06268663 0.04906305	b0.0218 b0.0077	0.203 0.076	0.40 0.44	0.7827
036	19 13 05.48 +12 38 02.2	14.97 - 15.66 ( <i>zg</i> )	C01	5.6242 3.9115	b1.36 b0.49	0.195 0.104	0.42 0.49	0.6955
037	19 15 27.55 +09 06 01.1	14.93 - 15.28 ( <i>zg</i> )	D12	0.1738900 0.1390354	b0.0180 b0.0206	0.086 0.060	0.48 0.47	0.7996
038	19 22 51.22 -59 07 05.4	14.40 - 14.72 ( <i>ag</i> )	D12	0.06644163 0.05312860	b0.0434 b0.0421	0.071 0.032	0.46 0.45	0.7996
039	19 24 06.38 +26 48 08.3	14.72 - 15.24 ( <i>zg</i> )	D012	0.1962641 0.1499660 0.1201920	b0.057 b0.063 b0.023	0.070 0.129 0.015	0.42 0.47 0.50	0.7641 0.8015
040	19 28 33.27 +23 29 20.2	14.87 - 15.37 ( <i>zg</i> )	C*12	0.345059 0.275878	b0.134 b0.047	0.178 0.024	0.50 0.47	0.7995
041	19 40 49.14 +27 36 13.3	15.50 - 16.01 ( <i>zg</i> )	D23	0.1608697 0.1327699	b0.0444 b0.0740	0.153 0.045	0.35 0.45	0.8253
042	19 44 01.74 +38 14 01.0	11.89 - 12.34 ( <i>ag</i> )	C*12	0.335738 0.268255	a0.268 a0.102	0.161 0.026	0.50 0.47	0.7990
043	19 59 00.10 +29 28 26.3	17.26 - 18.06 ( <i>zr</i> )	C01	0.840380 0.617996	b0.410 b0.460	0.127 0.117	0.34 0.40	0.7354
044	20 02 56.86 +23 20 32.1	11.73 - 12.05 ( <i>ag</i> )	D12	0.1769232 0.1405731	b0.1637 b0.0410	0.104 0.021	0.44 0.45	0.7945

**Table 1 (continued)**

MMRP	J2000	Magn.	Type	Period	Epoch	Ampl.	M-m	$P_S/P_L$
045	20 05 50.64 +30 58 57.3	12.73 - 13.02 ( <i>zg</i> )	D23	0.09904520 0.08253105	b0.0340 b0.0415	0.089 0.029	0.43 0.47	0.8333
046	20 08 29.64 +30 59 48.9	18.16 - 18.64 ( <i>zr</i> )	C12	0.662711 0.530568	b0.470 b0.175	0.147 0.022	0.42 0.46	0.8006
047	20 35 44.04 +47 50 35.7	17.60 - 18.09 ( <i>zr</i> )	C12	0.702280 0.566057	b0.009 b0.473	0.151 0.033	0.47 0.44	0.8060
048	20 57 52.03 +49 27 23.5	17.80 - 18.20 ( <i>zr</i> )	C12	0.533432 0.427953	b0.235 b0.046	0.135 0.031	0.47 0.45	0.8023
049	22 38 26.91 +43 52 49.4	13.96 - 14.43 ( <i>zg</i> )	D01	0.1794143 0.1375285	a0.1080 a0.1310	0.047 0.156	0.45 0.57	0.7665
050	23 47 49.26 +64 21 47.4	16.55 - 17.34 ( <i>zg</i> )	C12	0.85364 0.68721	b0.470 b0.568	0.227 0.058	0.39 0.44	0.8050

**Table 1a. Known multi-mode variables**

MMRP_J	Magn.	Type	Period	Epoch	Ampl.	M–m	$P_S/P_L$
044322.93+465703.6	14.75 – 15.58 ( <i>zg</i> )	C12	0.975593 0.782620	b0.165 b0.754	0.261 0.062	0.34 0.50	0.8022
054223.13+275647.6	12.89 – 13.61 ( <i>ag</i> )	C*12m	0.376512 0.300892	b0.217 b0.170	0.251 0.042	0.49 0.46	0.7992 –
074438.61+291222.8	11.94 – 12.53 ( <i>ag</i> )	D01	0.0885372 0.0684971	b0.0420 b0.0390	0.224 0.013	0.32 0.45	0.7737
093044.09+320916.8	15.67 – 16.53 ( <i>zg</i> )	R01	0.504562 0.375771	b0.165 b0.199	0.141 0.213	0.41 0.40	0.7447
094051.03+345205.2	14.44 – 15.34 ( <i>zg</i> )	R01	0.4598247 0.3415975	b0.183 b0.050	0.170 0.202	0.37 0.38	0.7429
105408.01–580421.2	14.52 – 15.03 ( <i>ag</i> )	D01	0.1932659 0.1475255	a0.0070 a0.1175	0.071 0.096	0.44 0.50	0.7633
111130.57–632636.4	12.66 – 13.00 ( <i>ag</i> )	D12n	0.15607022 0.1247588	a0.1060 a0.0460	0.088 0.046	0.43 0.48	0.7994
143130.85+225023.4	15.48 – 16.15 ( <i>zg</i> )	R01	0.4952015 0.3691332	b0.124 b0.033	0.067 0.217	0.48 0.39	0.7454
151609.22+320007.3	15.70 – 16.73 ( <i>zg</i> )	R01	0.4706323 0.3499155	b0.130 b0.224	0.193 0.232	0.39 0.37	0.7435
160331.49–494754.4	13.86 – 14.46 ( <i>ag</i> )	D012	0.2194880 0.1668487 0.1334800	b0.0400 b0.0615 b0.1111	0.068 0.161 0.013	0.45 0.54 0.50	0.7602 0.8000
171059.14–351034.8	14.09 – 14.40 ( <i>ag</i> )	D01	0.1232822 0.09510855	a0.0095 a0.0040	0.019 0.083	0.49 0.66	0.7715
185513.28+081813.4	17.43 – 18.28 ( <i>zr</i> )	C01	1.86705 1.34230	b0.16 b0.46	0.190 0.084	0.28 0.43	0.7189
202946.51+374539.5	14.65 – 15.31 ( <i>zr</i> )	C01	4.2972 2.9905	b4.08 b2.07	0.179 0.070	0.35 0.45	0.6959
211839.91+504732.9	15.09 – 16.09 ( <i>zg</i> )	C01	2.99683 2.11870	b0.35 b2.07	0.423 0.023	0.26 0.50	0.7070

**Table 2. Comments for new MMRP variables**

MMRP	Comments	MMRP	Comments
001	1,2,3	026	13,15,29,42
002	1,4,5	027	4,5,43,44
003	1,2,6	028	13,16,45,46
004	5,7	029	13,47,48
005	1,5,8,9,10,11	030	12,13,15,49
006	1,2,6,12	031	13,29,35,50
007	13,14,15,16,17	032	5,13,51
008	5,7,9,12	033	13,25,52
009	7,9,16,18,19,20	034	13,14,15,23
010	9,16,21,22	035	13,53
011	4,5,20,21,23,24	036	21,34,54,55,56,57
012	13,15,25	037	10,13,14,15,29
013	1,26	038	13,15,29
014	12,27	039	13,14,15,29,31,58
015	13,16,28,29	040	1,4,5,34
016	13,30	041	14,15,16,29
017	1,2,6,16	042	4,5,31,59
018	13,15,29,31	043	7,18,60
019	13,15,25,29,32,33	044	13,15,25,61
020	13,15,29,34	045	10,13,14,15,62
021	29,35,36,37	046	5,7,63
022	13,15,17,29,38	047	7,64
023	13,17,29,39	048	7,18,65
024	13,15,29,40	049	13,14,15,16,29,66
025	12,41	050	7,18,67

**Table 2a. Comments for known multi-mode variables**

MMRP_J	Comments
044322.93+465703.6	5,16,68,69
054223.13+275647.6	5,9,16,70,71
074438.61+291222.8	13,14,15,23,72
093044.09+320916.8	1,4,16,45,73,74,75
094051.03+345205.2	4,7,10,17,45,74,76,77
105408.01-580421.2	13,15,79
111130.57-632636.4	13,15,35,79,80
143130.85+225023.4	1,2,4,16,45,73,77,81,82
151609.22+320007.3	1,4,10,45,74,76,77,83
160331.49-494754.4	13,29,35,79,84
171059.14-351034.8	13,29,79,85
185513.28+081813.4	68,69
202946.51+374539.5	55,56,68,69,85
211839.91+504732.9	34,55,68,69,86

Comments.

1. Monoperiodic RRC in ZTF Catalog (Chen et al., 2020).
2. Monoperiodic RRC in Gaia DR3 Catalog (Gaia Collaboration, 2022).
3. MMRP–001. Large amplitude modulation of the second-overtone mode  $f_2$ . The amplitudes in the Table are for the first interval of ZTF observations, JD 2458219–2458540; for the next observation interval, JD 2458607–2459766, the amplitudes of the oscillations are as follows:  $f_1$ : A/2 is 0.109 (zr), 0.161 (zg);  $f_2$ : A/2 is 0.006 (zr), 0.011 (zg).
4. Monoperiodic RRC in ASAS-SN Catalog (Jayasinghe et al., 2018, 2019a, 2019b, 2020, 2021).
5. Monoperiodic first-overtone DCEP in Gaia DR3 Catalog.
6. Monoperiodic RRC in Gaia DR2 Catalog (Gaia Collaboration, Brown, et al., 2018).
7. Monoperiodic RRAB in ZTF Catalog.
8. Monoperiodic RRc in GCVS (Samus et al., 2017).
9. Monoperiodic RRAB in ASAS-SN Catalog.
10. Variable in ATLAS catalog (Heinze et al., 2018). Class of variability “MSINE” (stars showing modulated sinusoids).
11. Monoperiodic RRC in the Czech Variable Star Catalogue (Skarka et al., 2017).
12. Variable in ATLAS catalog. Class of variability “dubious” (the star might not be a real variable).
13. Monoperiodic HADS in ASAS-SN Catalog.
14. Monoperiodic DSCT in ZTF Catalog.
15. Monoperiodic “main-sequence oscillator”, or “DSCT/GDOR/SXPHE” type, in Gaia DR3 Catalog.
16. Variable in ATLAS catalog. Class of variability “MPULSE” (stars showing modulated pulsations).
17. Data from 1SWASP were used to improve the light elements.
18. Monoperiodic RRAB in Gaia DR3 Catalog.
19. MMRP–009. The light elements for the 1SWASP data:  

$$f_1: \text{HJD(max)} = 2454420.373 + 0^{\text{d}}48136 \times E;$$
  

$$f_2: \text{HJD(max)} = 2454420.240 + 0^{\text{d}}38565 \times E.$$
20. Blend in 1SWASP data.
21. Monoperiodic variable in ZTF suspected variables catalog (Chen et al., 2020). Type not determined.
22. MMRP–010. Equidistant quadruplet in fact:  $f_1 - f_0 = 1.006209$ ,  $f_2 - f_1 = 1.006210$ ,  $f_3 - f_2 = 1.006216$ .
23. Variable in ATLAS catalog. Class of variability “PULSE” (pulsating stars showing the classic sawtooth light curve, regardless of period).
24. MMRP–011. Light elements for the 1SWASP data:  

$$f_1: \text{HJD(max)} = 2454100.165 + 0^{\text{d}}37202 \times E;$$
  

$$f_2: \text{HJD(max)} = 2454100.011 + 0^{\text{d}}29826 \times E;$$
25. Monoperiodic DSCT in ASAS-3 Catalog of Variable Stars, Pojmanski (2002).
26. RR Lyrae star (RR) in Gaia DR3 Catalog.
27. HADS(B) star in VSX database. Period of the dominating mode is given, a second period is not given.
28. Monoperiodic EW star in ZTF Catalog.
29. Monoperiodic “short-timescale source” in Gaia DR3 Catalog.
30. MMRP–016. Amplitude modulation of the second-overtone mode,  $f_2$ . The Tables give mean amplitude (for the whole observation interval). Mode-switching is not excluded, type D12→D1. In  $g$  band, three time intervals were studied:

- I: JD 2458100–2458700,  $A = 0.036$ ;
- II: JD 2458700–2459400,  $A = 0.014$ ;
- III: JD 2459400–2459966,  $A \geq 0.007$ .

31. Variable in ATLAS catalog. Class of variability “CBF” (close binary, full period).
32. Monoperiodic eclipsing variable in the Catalina Surveys Southern periodic variable star catalogue (Drake et al., 2017).
33. MMRP-019. Amplitude modulation of the second-overtone mode,  $f_2$ . Periods  $P_1$  and  $P_2$  possibly vary, the light elements are given separately for two time intervals, for the  $V$  band (JD 2456776–2458382) and  $g$  band (JD 2458031–2460049). Elements for  $V$ -band ASAS-SN data:

$$\begin{aligned}f_1: \text{HJD(max)} &= 2457777.1590 + 0^d1633823 \times E; \\f_2: \text{HJD(max)} &= 2457777.1350 + 0^d1303228 \times E.\end{aligned}$$

34. Variable in ATLAS catalog. Class of variability “IRR” (irregular variable).
35. Variability was detected in the GDS catalog (Hackstein et al., 2015).
36. Monoperiodic SR variable in ASAS-SN Catalog.
37. MMRP-021. A second identification in the USNO-B1.0 catalog is possible, USNO-B1.0 0366-0148328.
38. MMRP-022. Additional non-radial pulsation with the following light elements, according to ASAS-SN data:

$$\begin{aligned}\text{for } V\text{-band, JD 2457424–2458326: HJD(max)} &= 2457878.083 + 0^d110475 \times E; \\ \text{for } g\text{-band, JD 2458282–2460046: HJD(max)} &= 2459292.100 + 0^d110468 \times E;\end{aligned}$$

$M - m = 0.48$ , period ratios  $P_n/P_1 = 0.7813$ ,  $P_n/P_0 = 0.5971$ . Semi-amplitudes  $A_n$  is 0.029 (aV), 0.029 (ag).

For the 1SWASP data: magnitude range  $14^m65$ – $15^m25$ ; amplitudes  $A_0 = 0.083$ ,  $A_1 = 0.074$ ,  $A_n = 0.014$ .

39. MMRP-023. According to 1SWASP data, semi-amplitudes are  $A_1 = 0.085$  and  $A_2 = 0.010$ .

40. MMRP-024. In the ASAS-SN  $g$ -band data, two possible non-radial modes with small amplitude are detected,  $f_n$  and  $f_m$ , periods  $P_n = 0^d109954$  and  $P_m = 0^d113563$ . Frequency  $f_n$  is also detected in 1SWASP data.

Amplitude modulation of all the radial modes. First overtone mode period varies. The light elements in the Table are for ASAS-SN  $g$ -band, JD 2458282–2460046. Elements for ASAS-SN  $V$ -band, JD 2457424–2458326:

$$\begin{aligned}f_0: \text{HJD(max)} &= 2457777.1520 + 0^d1828469 \times E; \\f_1: \text{HJD(max)} &= 2457777.1053 + 0^d1401100 \times E; \\f_2: \text{was not detected.}\end{aligned}$$

Elements for 1SWASP data, JD 2453860–2454239:

$$\begin{aligned}f_0: \text{HJD(max)} &= 2454141.083 + 0^d182847 \times E; A_0 = 0.077; \\f_1: \text{HJD(max)} &= 2454141.031 + 0^d140108 \times E; A_1 = 0.094; \\f_2: \text{HJD(max)} &= 2454141.111 + 0^d112110 \times E; A_2 = 0.009.\end{aligned}$$

Magnitude range  $13^m44$  –  $13^m98$  (1SWASP mag).

41. MMRP-025. Was detected as a candidate RR Lyrae star by Ivezić et al. (2000), [IGF2000] 4.

42. Monoperiodic DSCT star in the Catalina Surveys Southern periodic variable star catalogue (Drake et al., 2017).

43. Monoperiodic RRC star in ASAS-3 Catalog.

44. MMRP-027. Elements for ASAS-3 data:

$$\begin{aligned}f_1: \text{HJD(max)} &= 2453333.307 + 0^d342260 \times E; A_1 = 0.085; \\f_2: \text{HJD(max)} &= 2453333.410 + 0^d273581 \times E; A_2 = 0.018;\end{aligned}$$

Magnitude range 11<sup>m</sup>24–11<sup>m</sup>57 (*V*).

45. Data from CSS and SSS were used to improve the light elements.

46. MMRP-028. According to SSS data, semi-amplitude  $A_0 = 0.144$ ,  $A_1 = 0.031$ .

Magnitude range 14<sup>m</sup>85–15<sup>m</sup>36 (CV).

47. RS Canum Venaticorum star (RS type) in Gaia DR3 Catalog.

48. MMRP-029. Periods vary. Light elements for ASAS-SN *g*-band are given in the Table. Elements for ASAS-SN *V*-band:

$$f_0: \text{HJD(max)} = 2457777.0160 + 0^d0961740 \times E;$$

$$f_1: \text{HJD(max)} = 2457777.0138 + 0^d0742619 \times E.$$

49. DSCT\_SXPHE star in Gaia DR2 Catalog.

50. MMRP-031. According to ASAS-SN *g*-band data, possible non-radial mode with  $P_n = 0^d157944$ , or amplitude modulation (Blazhko effect) of the third-overtone mode with the period  $\Pi = 42^d$ .

51. MMRP-032. Amplitude modulation of the second-overtone mode  $f_2$ , mean amplitudes (for the full time-interval) are given in the Table. Three time intervals were studied:

I: JD 2458231–2458777,  $A = 0.009$ ;

II: JD 2458892–2459510,  $A = 0.030$ ;

III: JD 2459610–2460050,  $A \geq 0.006$ .

52. MMRP-033. Periodic variable of ambiguous classification, as given in Nataf et al. (2010). In OGLE catalog, possible wrong identification with OGLE-BLG-DSCT-06966.

Amplitude modulation of first overtone mode  $f_1$  is detected in the ASAS-SN data, *V* and *g* bands. The mean amplitudes are given in the Tables (for the whole observation intervals for individual bands).

Data from ASAS-3 were used to improve the light elements. Magnitude range and amplitude according to ASAS-3 data: 11<sup>m</sup>61–12<sup>m</sup>31 (*V*),  $A_0 = 0.217$ ,  $A_1 = 0.037$ .

53. MMRP-035. Data from SSS were used to improve the light elements of fundamental mode,  $f_0$ . First-overtone period  $P_1$  varies. Magnitude range and amplitude according to SSS data: 14<sup>m</sup>98–15<sup>m</sup>64 (CV),  $A_0 = 0.151$ ;  $A_1 = 0.073$ .

54. Monoperiodic rotational variable (ROT type) in ASAS-SN Catalog.

55. Monoperiodic fundamental mode  $\delta$  Cephei star (DCEP type) in Gaia DR3 Catalog.

56. MIRA\_SR variable in Gaia DR2 Catalog.

57. MMRP-036. Blend in NSVS and ASAS-SN data. Large magnitude scattering in ZTF *r*-band data. Elements for NSVS data:

$$f_0: \text{HJD(max)} = 2451402.91 + 5^d61 \times E; A_0 = 0.068;$$

$$f_1: \text{HJD(max)} = 2451401.55 + 3^d91 \times E; A_1 = 0.025;$$

Magnitude range 12<sup>m</sup>09–12<sup>m</sup>34 (*R*).

58. MMRP-039. In *V*-band ASAS-SN data, JD 2456084–2458427 (earliest time-interval), second-overtone mode  $f_2$  is not detected, semi-amplitude  $A_2 > 0.014$ . Possibly, it is due to large errors, or amplitude modulation is possible.

59. The variability was detected by Hartman et al. (2004), pulsating type.

60. MMRP-043. In the ZTF catalog, two periods were detected: for the *r* band,  $P = 0^d8404704$  corresponds to  $f_0$  (the most likely period), or for the *g*-band,  $P = 0^d6179089$  corresponds to  $f_1$ .

61. Variable in ATLAS catalog. Class of variability “SINE” (sinusoidal variables).

62. Monoperiodic DSCT star in GCVS.

63. Monoperiodic RRAB star in Gaia DR2 Catalog.

64. MMRP-047. Amplitude and magnitude range in the *i* band of ZTF data:  $A_1 = 0.115$ ,  $A_2 = 0.026$ ; 16<sup>m</sup>64–16<sup>m</sup>98 (*i*).

65. MMRP-048. Amplitude and magnitude range in the  $i$  band of ZTF data:  $A_1 = 0.101$ ,  $A_2 = 0.024$ ;  $16^m 73 - 17^m 04$  ( $i$ ).

66. MMRP-049. Elements for 1SWASP data:

$$f_0: \text{HJD(max)} = 2454345.442 + 0^d 17941 \times E; A_0 = 0.033;$$

$$f_1: \text{HJD(max)} = 2454345.531 + 0^d 13753 \times E; A_1 = 0.103.$$

Magnitude range  $14^m 00 - 14^m 46$  (1SWASP mag).

67. MMRP-050. Periods  $P_1$  and  $P_2$  possibly vary.

68. Monoperiodic DCEP variable in ZTF Catalog.

69. Multiperiodicity detected by Shah et al. (2022).

70. Monoperiodic RRAB star in GCVS.

71. MMRP\_J054223.13+275647.6 = IY Tau. Double periodicity was detected by Khruslov (2018)<sup>11</sup>. In this study, I detected amplitude modulation of the second-overtone mode  $f_2$ , according to ASAS-SN data. The Table gives semi-amplitude for the second  $g$ -band interval, JD 2459429–2460055. For the first  $g$ -band interval, JD 2458083–2459328,  $A_1 = 0.274$ ,  $A_2 = 0.018$ . Period  $P_1$  varies. For the  $V$ -band, ASAS-SN data gives the following elements:

$$f_1: \text{HJD(max)} = 2457777.140 + 0^d 376502 \times E;$$

$$f_2: \text{HJD(max)} = 2457777.283 + 0^d 300891 \times E;$$

$V$ -band amplitudes in Tables are given according to data from the second  $V$ -band interval, JD 2457745–2458443. Amplitude for the first  $V$ -band interval, JD 2457008–2457720:  $A_1 = 0.212$ ,  $A_2 \geq 0.006$  ( $f_2$  is not detected);

Elements according to 1SWASP data (for light curves see Khruslov, 2018):

$$f_1: \text{HJD(max)} = 2453777.214 + 0^d 3764978 \times E; A_1 = 0.168;$$

$$f_2: \text{HJD(max)} = 2453777.096 + 0^d 3009072 \times E; A_2 = 0.028.$$

72. MMRP\_J074438.61+291222.8. Double periodicity was detected by Wils et al. (2012), classified as a HADS star of fundamental and first-overtone modes. Periods vary. Light elements in the Table are given for the time interval JD 2458033–2459830, ASAS-SN  $g$  band and ZTF  $g$  band.

For ASAS-SN  $V$ -band, JD 2456905–2458452, light elements are:

$$f_0: \text{HJD(max)} = 2457777.0787 + 0^d 0885367 \times E;$$

$$f_1: \text{HJD(max)} = 2457777.0090 + 0^d 0684978 \times E;$$

Elements for 1SWASP data:

$$f_0: \text{HJD(max)} = 2454120.0653 + 0^d 0885370 \times E; A_0 = 0.188;$$

$$f_1: \text{HJD(max)} = 2454120.0228 + 0^d 0684974 \times E; A_1 = 0.016.$$

73. Double-mode RR Lyrae star (RRd type) in Gaia DR2 Catalog.

74. Double-mode RR Lyrae star (RRd type) in Gaia DR3 Catalog.

75. MMRP\_J093044.09+320916.8. Magnitude range and semi-amplitude according to CSS data:  $15^m 65 - 16^m 34$  (CV);  $A_0 = 0.112$ ,  $A_1 = 0.167$ .

76. Double-mode RR Lyrae variable (RRd type) in the Catalina Surveys periodic variable stars catalog (Drake et al., 2014).

77. Double periodicity detected by Huemmerich and Bernhard (2014) corresponds to 2012. Type RRd.

78. MMRP\_J094051.03+345205.2 Magnitude range and semi-amplitude:

according to CSS data:  $14^m 43 - 15^m 15$  (CV);  $A_0 = 0.135$ ,  $A_1 = 0.152$ ;

according to 1SWASP data:  $14^m 6 - 15^m 6$  (1SWASP mag),  $A_0 = 0.164$ ,  $A_1 = 0.192$ .

79. The variable is in the OGLE  $\delta$  Scuti stars database<sup>12</sup>, Pietrukowicz et al. (2020).

<sup>11</sup> <http://www.inasan.ru/wp-content/uploads/2018/12/Boyarchuk.pdf#page=57>

<sup>12</sup> [https://ogledb.astrow.u.edu.pl/ogle/OCVS/dsct\\_query.php](https://ogledb.astrow.u.edu.pl/ogle/OCVS/dsct_query.php)

80. MMRP\_J111130.57–632636.4. According to ASAS-SN  $g$ -band data, there is additional non-radial oscillation,  $P_n = 0^d12072463$ ;  $A_n = 0.008$ .
81. Monoperiodic RRC star in the Catalina Surveys periodic variable stars catalog (Drake et al., 2014).
82. MMRP\_J143130.85+225023.4. Magnitude range and semi-amplitude according to CSS data:  $15^m35\text{--}15^m92$  (CV),  $A_0 = 0.040$ ,  $A_1 = 0.172$ .
83. MMRP\_J151609.22+320007.3. Magnitude range and semi-amplitude according to CSS data:  $15^m76\text{--}16^m51$  (CV),  $A_0 = 0.117$ ,  $A_1 = 0.155$ .
84. MMRP\_J160331.49–494754.4. Second-overtone mode  $f_2$  is not detected in ASAS-SN  $V$ -band.  
Possible non-radial oscillation  $f_n$  detected in ASAS-SN  $g$  and  $V$  bands,  $P_n = 0^d1262036$ ,  $A_n = 0.012$  (ag); this frequency is possibly a one-day alias mode to third overtone mode,  $f_n = f_3 - 1$ .  
In ASAS-SN  $V$ -band, two other oscillation with the periods close to  $P_1$ ,  $0^d1345739$  and  $0^d1349735$ , are possibly detected.
85. Blend in ASAS-SN data.
86. Monoperiodic DCEP star in ASAS-SN Catalog.

## 5.2 Light curves

An example of light curves for one of the stars, MMRP-049, is displayed in Fig. 1. Top panels present data folded with the fundamental-mode and first-overtone periods. Bottom panels show the same curves after prewhitening the other oscillation (if  $f_1+f_0$ ,  $f_1-f_0$  and  $f_1+2f_0$  interaction frequencies or non-radial frequencies were excluded, it is also noted). Along with the light curves, we present power spectra of the double-mode variables, for the raw data and after subtraction of the dominant mode (first-overtone oscillations for MMRP-049). The structure of the power spectra shows that the secondary periods are real.

The light curves from the ASAS-SN surveys are available online in the html version of this paper as a zip archive (see Section 2). The light curves are given in the format displayed in Fig. 1. A similar and more complete format is used for triple- and quadruple-mode variables.

## 6 Discussion

### 6.1 The Petersen diagram

Among the 50 stars with multi-periodicity discovered in this study, there are 15 Classical Cepheids (two stars of the C01 type, 8 stars of the C12 type, and 5 stars of the C\*12 type); four RR Lyrae stars of the R01 type; 31 high-amplitude  $\delta$  Scuti stars (double-mode: 9 D01 stars, 12 D12 stars, 4 D23 stars; triple-mode: 4 D012 stars and one D123 star; and one quadruple-mode star of the D0123 type).

Among the 14 known multi-periodic stars studied in this paper, there are 5 Classical Cepheids (three of C01 type, one of C12 type, and one of C\*12 type); four RR Lyrae stars of R01 type; 5 high-amplitude  $\delta$  Scuti stars (3 of D01 type, one of D12 type, one of D012 type).

In this paper, the distribution by variability type is not statistically significant. In fact, in the sample of multi-periodic variable stars, the largest fraction belongs to R01 stars. The number of D01 stars is slightly lower. Next in number are the first- and

J2000: 22 38 26.91 +43 52 49.4      MMRP-049

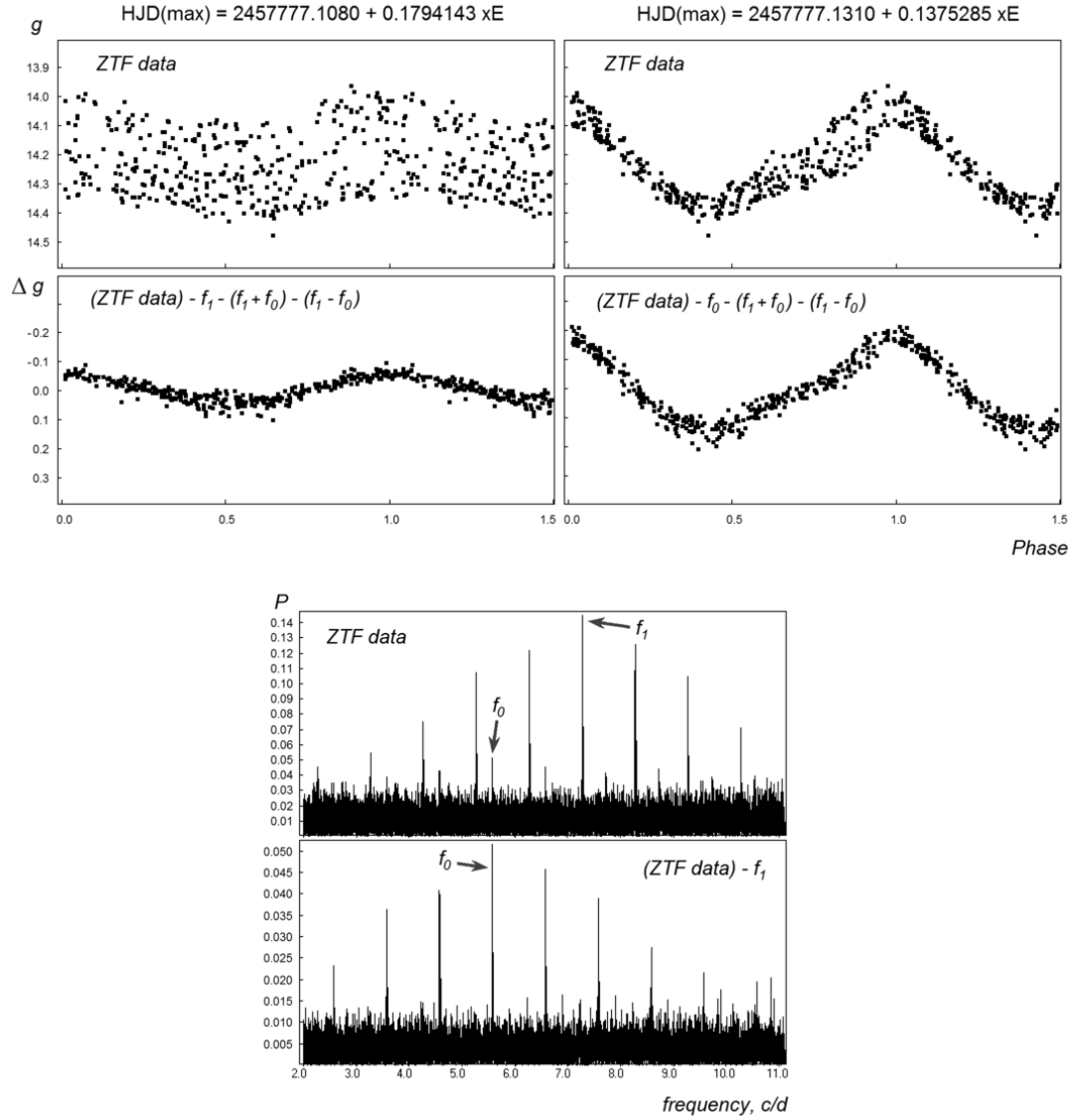


**Figure 1.**

The light curves and power spectra of the star MMRP-049 (D01 type) from  $g$ -band ASAS-SN data.

second-overtone variables of different types (D12 and C12) and C01 Cepheids. For the present paper, I selected the rarest and most interesting objects encountered in my search for multi-periodicity.

The Petersen diagram for all MMRP variables studied in this paper is displayed in Fig. 2.

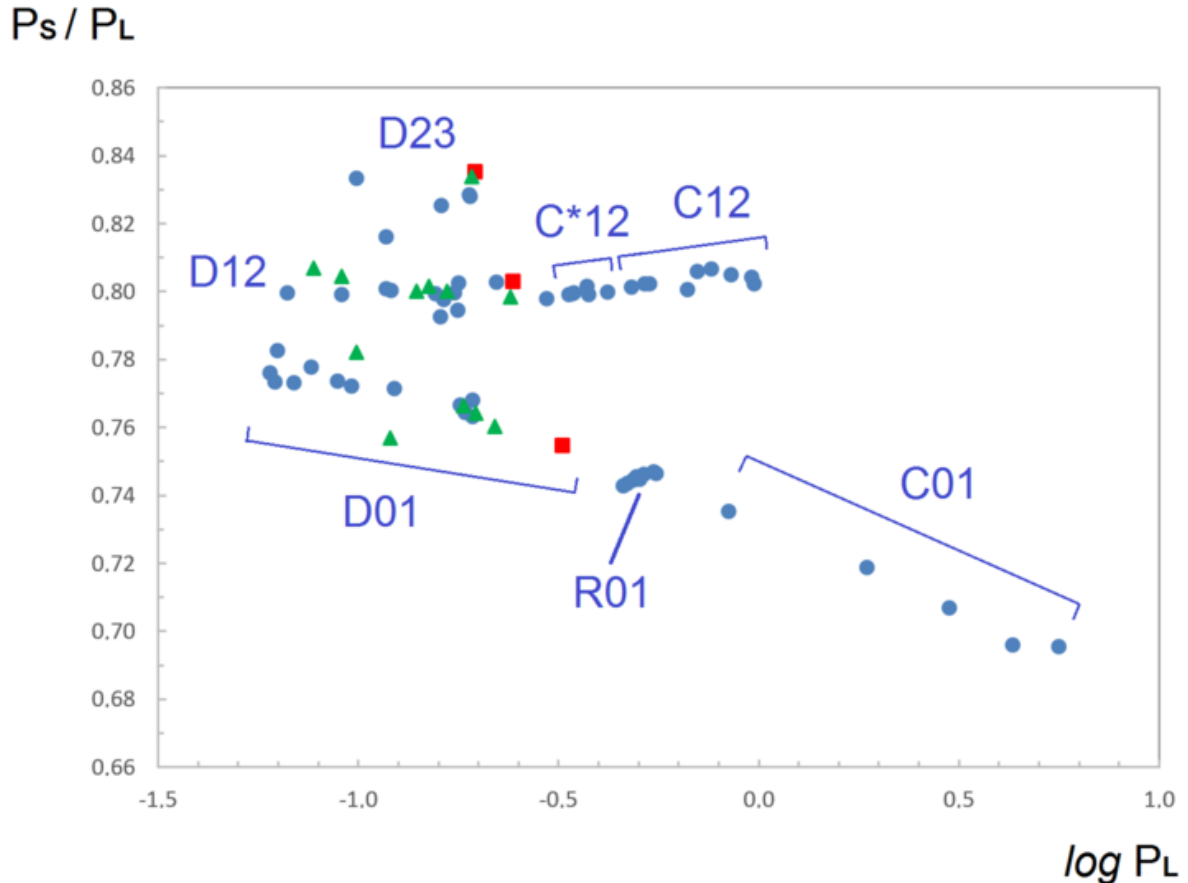


**Figure 2.**

The Petersen diagram for the multi-periodic stars of the present study. Blue circles are double-mode variables, green triangles are triple-mode variables, and red squares are quadruple mode variables.

## 6.2 Asymmetry inversion for light curves of $\delta$ Scuti stars

In the photometric data of recent surveys, we find more and more  $\delta$  Scuti stars with light-curve asymmetry opposite compared to brightness variations of typical pulsating stars. Pietrukowicz et al. (2020) show four examples of phased light curves of monoperiodic  $\delta$  Scuti variables with inversion of asymmetry (the rising part lasting longer than the fading one), and classify these stars as likely first-overtone pulsators.

In this paper, I present a confirmation of this assumption using multiperiodic stars. I detected 10 double- and multi-mode variables with one of the modes showing asymmetry inversion. Among these stars, three are of the D01 type (MMRP–22, MMRP–49, and MMRP\_J171059.14–351034.8), four stars belong to the D12 type (MMRP–19, MMRP–23, MMRP–26, and MMRP–32), two stars are of the D012 type (MMRP–24 and

MMRP\_J160331.49–494754.4), and one star is of the D0123 type (MMRP–10). In all these cases, the mode with asymmetry inversion is the first overtone.

An example of the light curves of one of the stars with asymmetry inversion (MMRP–49) is shown in Fig. 1.

The maximal asymmetry inversion was detected for MMRP\_J171059.14–351034.8,  $M - m = 0^{\circ}66$ .

All these stars have the longest periods for  $\delta$  Scuti stars,  $0^{\text{d}}296 > P_1 > 0^{\text{d}}095$  (for four monoperiodic cases by Pietrukowicz et al., 2020, the periods are within the range  $0^{\text{d}}130 > P_1 > 0^{\text{d}}087$ ).

In addition, a slight inversion of asymmetry was detected for MMRP–011, a star of the C\*12 type ( $M - m = 0.52$ ). MMRP–011 ( $P_1 = 0^{\text{d}}372$ ,  $b = +0^{\circ}.9$ ) is similar to the D12 star MMRP–032 ( $P_1 = 0.296$ ,  $b = +2^{\circ}.0$ ) and to two known double-mode first- and second-overtone variables with a slight inversion of asymmetry, V798 Cyg ( $P_1 = 0^{\text{d}}195$ ,  $b = +4^{\circ}.6$ ) and V1719 Cyg ( $P_1 = 0^{\text{d}}267$ ,  $b = +2^{\circ}.6$ ). Note both the morphological similarity of the light curves and the stars' similar position relative to the Galactic plane.

### 6.3 C\*12 stars

In addition to the C12 type, I used the C\*12 type that includes stars morphologically close to the C12 type (asymmetry parameter  $M - m = 0.50$  or slightly inverted asymmetry, with a small hump at the beginning of the brightness increase), but with shorter periods ( $0^{\text{d}}45 > P_1 > 0^{\text{d}}30$ ) characteristic of R1 stars (RRC), bordering  $\delta$  Scuti stars. All these stars are located near the Galactic plane. This classification is based on OGLE<sup>13</sup> and Gaia DR3 catalogs (Gaia Collaboration, 2022), which classified similar stars as first- and second-overtone Cepheids. In my study, 6 stars belong to the C\*12 type: MMRP005, MMRP011, MMRP027, MMRP040, MMRP042, and MMRP\_J054223.13+275647.6 = IY Tau.

It should be noted that in the OGLE classification (see Soszyn'ski et al., 2020), a number of stars from the MMRP list with even shorter periods (of  $\delta$  Scuti type in my classification) are attributed to first-overtone Cepheids (MMRP002 and MMRP032). Some other variables may also be related to this type of stars (MMRP001 and MMRP010).

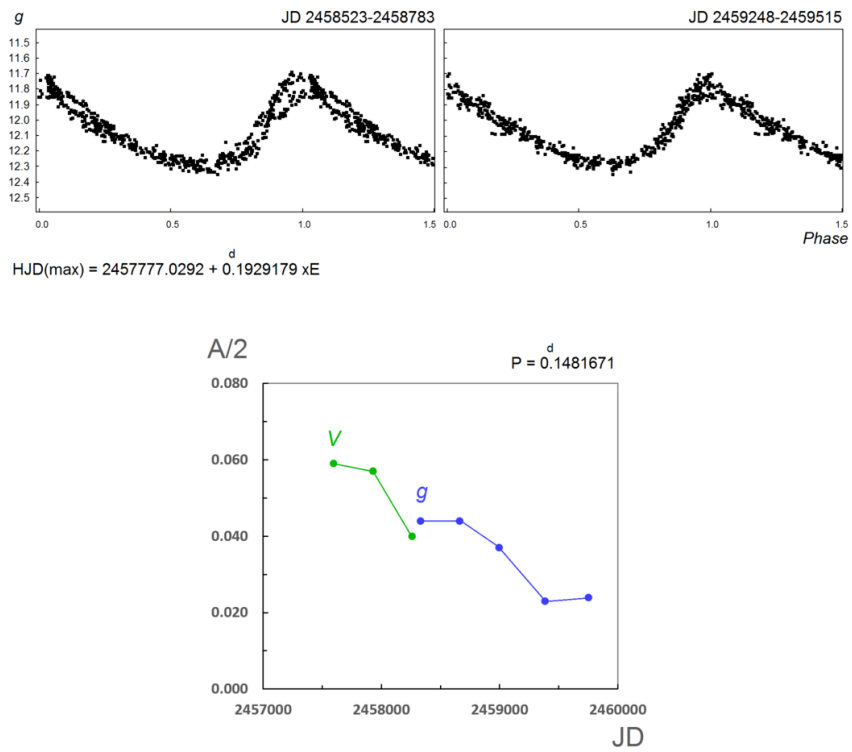
### 6.4 Amplitude modulation

For 7 variables, slow amplitude modulation (variations from one season to another) was detected. For these stars, the tabulated variability type included the letter "m" (for example, C12m, D12m, D01m). These are mainly cases of amplitude modulation of the second-overtone mode for the first- and second-overtone double-mode  $\delta$  Scuti variables (four D12m type stars: MMRP–001, MMRP–16, MMRP–19, and MMRP–32). One D01m star (MMRP–33) showed amplitude modulation of the first-overtone mode. One triple-mode  $\delta$  Scuti star of type D012m (MMRP–24) showed possible amplitude modulation of all its radial pulsation modes. Also, one C\*12m Cepheid star, MMRP\_J054223.13+275647.6 = IY Tau, showed amplitude modulation of the second-overtone mode.

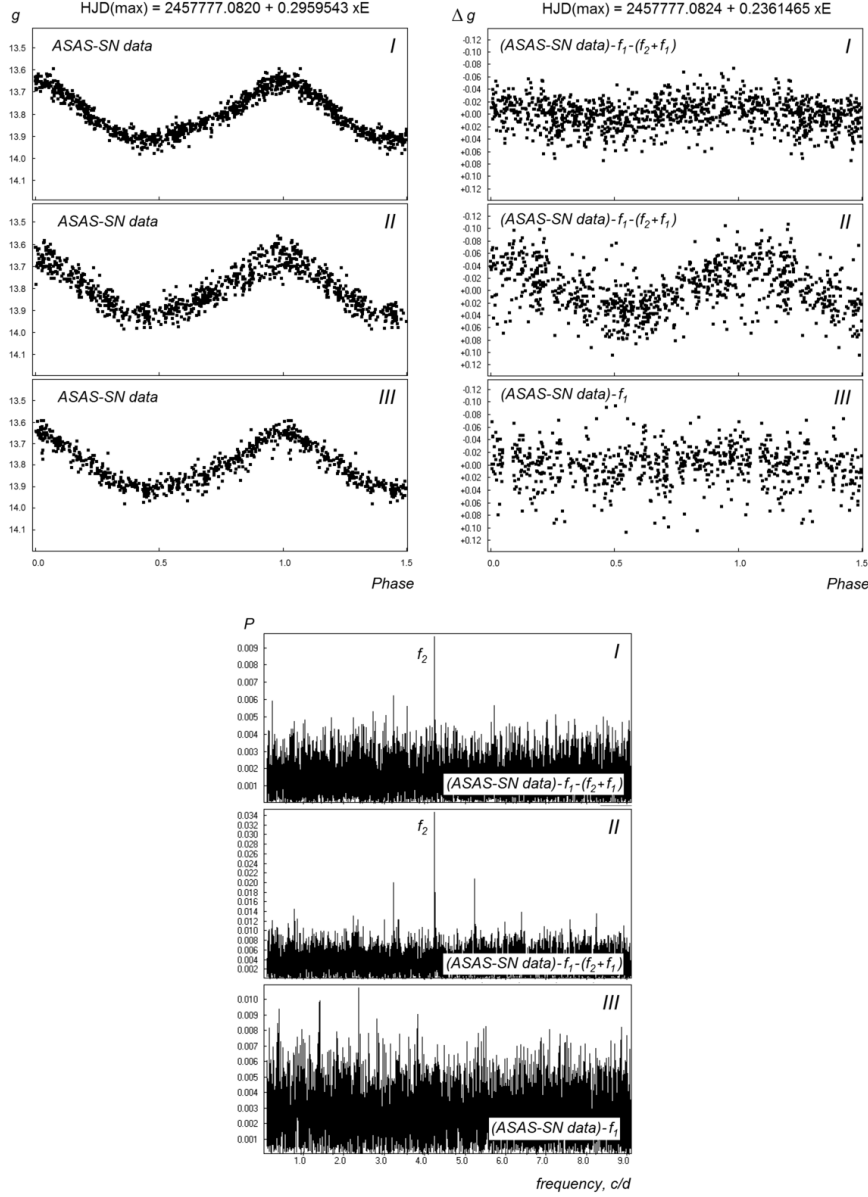
In some cases, a periodic amplitude variation is possible, but, in a number of cases, it also can be mode switching.

Two examples of amplitude modulation are shown in Figs. 3 and 4. MMRP–033 is a possible mode-switching case. MMRP–032 is possibly a case of periodic amplitude variations (during short time intervals of observations, the star shows the "episodic" multiperiodicity; for intervals and variability amplitudes, see Comments to Table 1).

<sup>13</sup> [https://ogledb.astroweb.edu.pl/ogle/OCVS/ceph\\_query.php](https://ogledb.astroweb.edu.pl/ogle/OCVS/ceph_query.php)

**Figure 3.**

The amplitude modulation of MMRP-033. Top panels:  $g$ -band ASAS-SN data folded with the fundamental-mode period  $P_0$  in the two time-intervals; Bottom panel: amplitude variations of the first-overtone mode in the  $g$  and  $V$  bands of ASAS-SN data.

**Figure 4.**

The amplitude modulation of MMRP-032 in three time intervals (see Comments). Left panels:  $g$ -band ASAS-SN data folded with the first-overtone mode period  $P_1$ ; right panels:  $g$ -band ASAS-SN data folded with the second-overtone mode period  $P_2$ ; bottom panel: the power spectra of the second-overtone mode.

## 6.5 Triple- and quadruple-mode $\delta$ Scuti stars

In my study, 6 triple-mode variables were detected. Five of these stars belong to the D012 type: MMRP-012, MMRP-014, MMRP-024, MMRP-039, MMRP\_J160331.49–494754.4. In the case MMRP\_J160331.49–494754.4, the second-overtone mode was not earlier known (in the OGLE database, the star was classified as a variable with two periods, those of the fundamental and first-overtone modes). The sixth star, MMRP-002, belongs to the D123 type.

In all cases of the five D012 stars, with a single exception of MMRP-014, the first-overtone mode dominates. The first-overtone mode also dominates for the D123 star MMRP-002. In two cases, the light curve of the first-overtone oscillation showed asymmetry inversion.

One case, MMRP-010, is a quadruple-mode  $\delta$  Scuti star of the D0123 type. Additionally, it is an equidistant quadruplet with the frequency differences  $f_1 - f_0 = f_2 - f_1 = f_3 - f_2 = 1.0062$ . The light curve of the first-overtone oscillation of this star also shows inverted asymmetry.

Netzel et al. (2022) presents 14 quadruple-mode  $\delta$  Scuti stars of the D0123 type from the OGLE database (Galactic bulge). Among them, no one is an equidistant quadruplet. These authors also presented the discovery of numerous triple-mode  $\delta$  Scuti star of the D013 type (221 variables), their number considerably exceeding that of the D012 stars (145 variables). In my study, no D013 stars were detected.

## 6.6 D23 variables

In this paper, I present my detection of four double-mode  $\delta$  Scuti stars pulsating in the second- and third-overtone modes, type D23 (MMRP-020, MMRP-031, MMRP-041, and MMRP-045 = V2702 Cyg). Earlier, I found two stars of this type. The first of them is FH Cir (Khruslov, 2010, first classification as a  $\delta$  Scuti star with nonradial pulsations;  $P_2 = 0^d1522950$ ,  $P_3/P_2 = 0.8279$ ; the star was reclassified as a D23 variable by Khruslov, 2016, PhD dissertation<sup>14</sup>). The second of them is V3124 Cyg (Khruslov, 2014,  $P_2 = 0^d1053020$ ,  $P_3/P_2 = 0.8342$ ).

According to my study, the second-overtone periods of D23 stars range from  $0^d099$  to  $0^d190$ . The period ratio  $P_3/P_2$  is from 0.8253 to 0.8342.

For one of the stars, MMRP-031, I detected an amplitude modulation of the third-overtone mode that can be interpreted as Blazhko effect with the period  $\Pi = 42^d$  or as a non-radial mode with a frequency close to that of the third-overtone mode,  $P_n = 0^d157944$ . This case can be possibly classified as a D23n star, where the letter “m” in the MMRP catalog designates long-term variations and is not used for stars with Blazhko effect.

It is particularly interesting that Netzel et al. (2022) did not detect any stars of the D23 type.

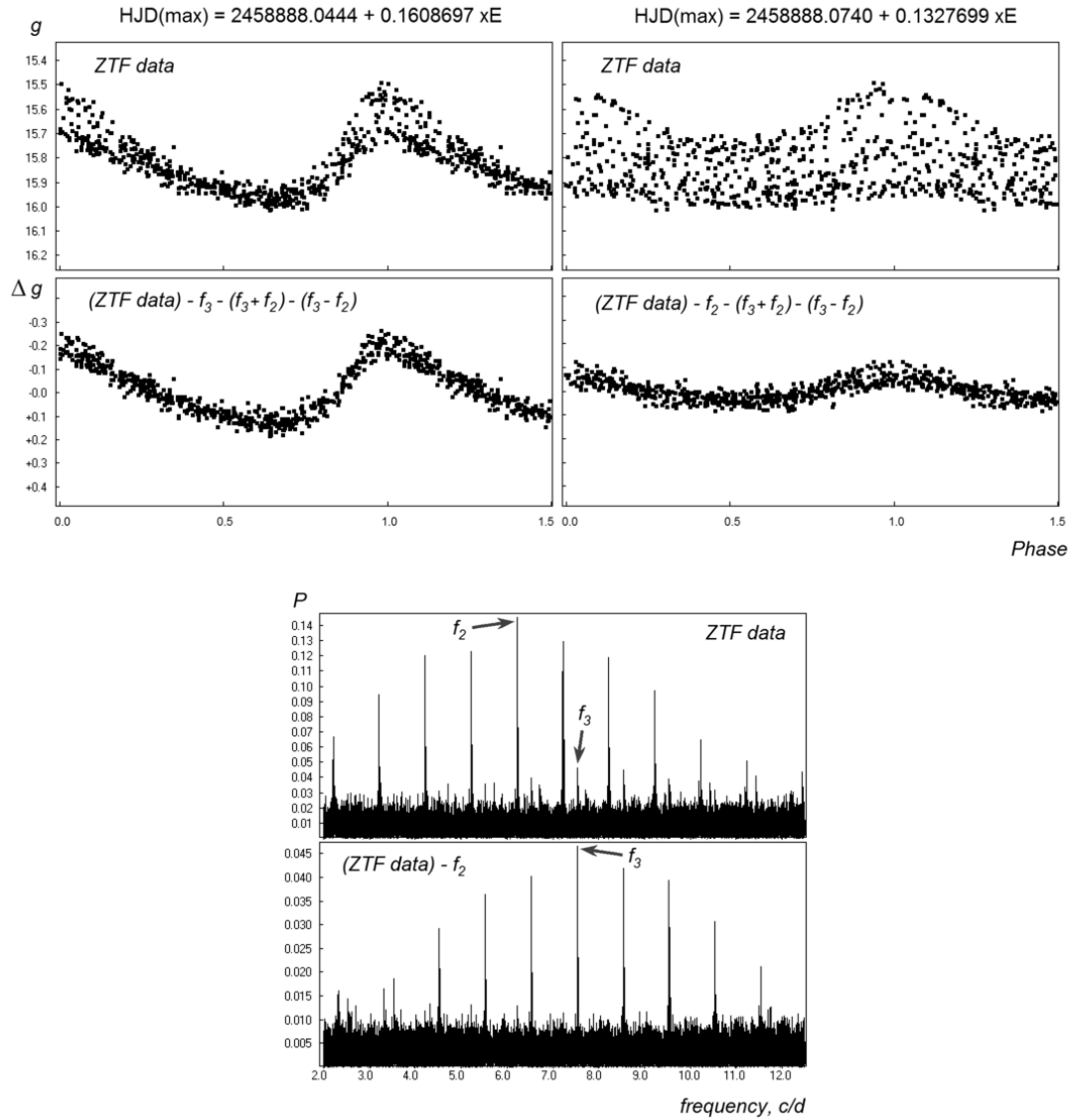
**Acknowledgments:** The author wishes to thank Dr. V.P. Goranskij for providing his software.

---

<sup>14</sup> [https://www.sai.msu.ru/dissovet/Khruslov\\_PhD.pdf](https://www.sai.msu.ru/dissovet/Khruslov_PhD.pdf)

J2000: 19 40 49.14 +27 36 13.3

MMRP-041

**Figure 5.**The light curves and power spectra of the star MMRP-041 (D23 type) from *g*-band ZTF data.

## References:

- Bellm, E. C., Kulkarni, S. R., & Graham, M. J., 2019, *Publ. Astron. Soc. Pacific*, **131**, 018002
- Butters, O. W., West, R. G., Anderson, D. R., et al. 2010, *Astron. & Astrophys.*, **520**, L10
- Chen, X., Wang, S., Deng, L., et al., 2020, *Astrophys. J. Suppl. Ser.*, **249**, id. 18
- Drake, A. J., Djorgovski, S. G., Mahabal, A., et al., 2009, *Astrophys. J.*, **696**, 870
- Drake, A. J., Graham, M. J., Djorgovski, S. G., et al., 2014, *Astrophys. J. Suppl.*, **213**, 9
- Drake, A. J., Djorgovski, S. G., & Catelan, M., 2017, *Monthly Notices Roy. Astron. Soc.*, **469**, 3688
- Gaia Collaboration, Brown, A.G.A., Vallenari, A., Prusti, T., et al., 2018, *Astron. & Astrophys.*, **616**, id. A1
- Gaia Collaboration, 2022, Gaia DR3 Part 4. Variability, VizieR On-line Data Catalog: I/358
- Hackstein, M., Fein, Ch., Haas, M., et al., 2015, *Astron. Nachr.*, **336**, 590
- Hartman, J.D., Bakos, G., Stanek, K.Z., & Noyes, R.W., 2004, *Astron. J.*, **128**, 1761
- Heinze, A. N., Tonry, J. L., Denneau, L., et al., 2018, *Astron. J.*, **156**, id. 241
- Huemmerich, S. & Bernhard, K., 2014, *Inform. Bull. Var. Stars*, No. 6100
- Ivezic, Ž., Goldston, J., Finlator, K., et al., 2000, *Astron. J.*, **120**, 963
- Jayasinghe, T., Kochanek, C. S., Stanek, K. Z., et al., 2018, *Monthly Notices Roy. Astron. Soc.*, **477**, 3145
- Jayasinghe, T., Kochanek, C. S., Stanek, K. Z., et al., 2021, *Monthly Notices Roy. Astron. Soc.*, **503**, 200
- Jayasinghe, T., Stanek, K. Z., & Kochanek, C. S., 2019a, *Monthly Notices Roy. Astron. Soc.*, **486**, 1907
- Jayasinghe, T., Stanek, K. Z., & Kochanek, C. S., 2019b, *Monthly Notices Roy. Astron. Soc.*, **485**, 961
- Jayasinghe, T., Stanek, K. Z., & Kochanek, C. S., 2020, *Monthly Notices Roy. Astron. Soc.*, **491**, 13
- Khruslov, A. V., 2010, *Perem. Zvezdy Prilozhenie (Variable Stars Suppl.)*, **10**, 15
- Khruslov, A. V., 2014, *Perem. Zvezdy Prilozhenie (Variable Stars Suppl.)*, **14**, 1
- Khruslov, A. V., 2016, *Detection and study of pulsating variable stars with multiperiodicity*, PhD Dissertation, Moscow: Moscow State University
- Khruslov, A. V., Kusakin, A. V., & Reva, I. V., 2017, *Acta Astron.*, **67**, 317
- Khruslov, A. V., 2018, Proceedings of the 2018 Acad. A. A. Boyarchuk Memorial Conference, INASAN Science Proceedings. Edited by D. V. Bisikalo and D. S. Wiebe. Moscow: Yanus-K, 2018, p. 57–61
- Khruslov, A. V., 2018a, *Perem. Zvezdy (Variable Stars)*, **38**, 1
- Khruslov, A. V., 2021, *Perem. Zvezdy (Variable Stars)*, **41**, 1
- Khruslov, A. V., 2021a, *Perem. Zvezdy (Variable Stars)*, **41**, 8
- Khruslov, A. V., 2022, *Perem. Zvezdy (Variable Stars)*, **42**, 5
- Kochanek, C. S., Shappee, B. J., Stanek, K. Z., et al., 2017, *Publ. Astron. Soc. Pacific*, **129**, 104502
- Malanchev, K. L., Pruzhinskaya, M. V., Korolev, V. S., et al., 2021, *Monthly Notices Roy. Astron. Soc.*, **502**, 5147
- Masci, F. J., Laher, R. R., & Rusholme, B., 2019, *Publ. Astron. Soc. Pacific*, **131**, 018003
- Nataf, D. M., Stanek, K. Z., & Bakos, G. Á., 2010, *Acta Astron.*, **60**, 261

- Netzel, H., Pietrukowicz, P., Soszyński, I., & Wrona, M., 2022, *Monthly Notices Roy. Astron. Soc.*, **510**, 1748
- Petersen, J. O., 1973, *Astron. & Astrophys.*, **27**, 89
- Petersen, J. O. & Christensen-Dalsgaard, J., 1996, *Astron. & Astrophys.*, **312**, 463
- Pietrukowicz, P., Soszyński, I., Netzel, H., et al., 2020, *Acta Astron.*, **70**, 241
- Pojmanski, G., 2002, *Acta Astron.*, **52**, 397
- Samus, N. N., Kazarovets, E. V., Durlevich, O. V., Kireeva, N. N., & Pastukhova, E. N., 2017, *Astron. Rep.*, **61**, 80
- Shah, V., Chen, X., & de Grijs, R., 2022, *Astron. J.*, **164**, 162
- Shappee B.J., Prieto J.L., Grupe, D., et al., 2014, *Astrophys. J.*, **788**, 48
- Skarka, M., Mašek, M., & Brát, L., 2017, *Open European Journal on Variable Stars*, **185**, p. 1
- Smolec, R. & Moskalik, P., 2010, *Astron. & Astrophys.*, **524**, A40
- Sokolovsky, K. V., 2007, *Perem. Zvezdy Prilozhenie (Variable Stars Suppl.)*, **7**, No. 30
- Soszyński, I., Udalski, A., Szymański, M. K., et al., 2020, *Acta Astron.*, **70**, 101
- Wils, P., Panagiotopoulos, K., van Wassenhove, J., et al., 2012, *Inform. Bull. Var. Stars*, No. 6015

## 7 Supplement Tables

**Table 3. Semi-amplitudes and magnitude ranges. New MMRP stars**

MMRP	Semi-ampl.				Mag. range			
	<i>aV</i>	<i>ag</i>	<i>zr</i>	<i>zg</i>	<i>aV</i>	<i>ag</i>	<i>zr</i>	<i>zg</i>
001	—	—	0.102	0.159	—	—	16.27–	17.12–
	—	—	0.046	0.060			16.66	17.63
002	0.125	0.147	0.100	0.149	14.87–	15.34–	14.55–	15.40–
	0.025	0.037	0.022	0.034	15.42	16.02	14.91	15.94
	0.032	0.042	0.029	0.039				
003	—	—	0.058	0.086	—	—	17.64–	17.73–
	—	—	0.150	0.224			18.20	18.47
004	0.139	0.155	0.150	0.230	15.15–	15.77–	14.74–	16.12–
	—	0.025	0.011	0.018	15.75	16.45	15.14	16.70
005	0.117	0.140	—	0.133	11.87–	12.26–	—	12.27–
	0.027	0.035	—	0.038	12.31	12.68		12.71
006	—	—	0.042	0.059	—	—	17.51–	17.66–
	—	—	0.162	0.238			18.00	18.41
007	0.107	0.109	0.076	0.118	13.86–	13.96–	13.86–	13.94–
	0.034	0.038	0.025	0.036	14.27	14.37	14.11	14.32
008	0.131	0.161	0.133	0.187	15.61–	16.20–	15.16–	16.47–
	0.051	0.061	0.045	0.066	16.38	17.08	15.58	17.09
009	0.206	0.254	0.165	0.257	13.98–	14.48–	13.54–	14.44–
	0.027	0.040	0.029	0.043	14.63	15.25	14.00	15.11
010	0.143	0.164	0.112	0.162	14.00–	14.37–	13.68–	14.32–
	0.120	0.136	0.102	0.130	14.74	15.21	14.26	15.17
	0.025	0.025	0.016	0.024				
	0.020	0.023	0.016	0.023				
011	0.132	0.163	0.128	0.193	13.44–	13.77–	13.34–	13.99–
	0.014	0.022	0.015	0.022	13.83	14.30	13.68	14.48
012	0.005	0.004	—	—	12.56–	12.66–	—	—
	0.187	0.228	—	—	13.04	13.24		
	0.013	0.018	—	—				
013	—	—	0.127	0.155	—	—	18.12–	18.92–
	—	—	0.155	0.199			18.81	19.88
014	—	—	0.133	0.208	—	—	16.65–	16.53–
	—	—	0.089	0.111			17.37	17.61
	—	—	0.023	0.036				

**Table 3 (continued)**

MMRP	Semi-ampl.				Mag. range			
	<i>aV</i>	<i>ag</i>	<i>zr</i>	<i>zg</i>	<i>aV</i>	<i>ag</i>	<i>zr</i>	<i>zg</i>
015	0.097	0.112	0.072	0.128	13.93–	14.12–	14.00–	14.11–
	0.029	0.033	0.020	0.032	14.24	14.48	14.24	14.50
016	0.164	0.200	–	–	14.01–	14.14–	–	–
	0.032	0.015	–	–	14.50	14.70		
017	–	–	0.047	0.069	–	–	16.17–	16.36–
	–	–	0.162	0.231			16.69	17.09
018	0.124	0.141	0.071	0.144	13.50–	13.68–	13.50–	13.68–
	0.015	0.027	0.013	0.023	13.86	14.10	13.74	14.05
019	0.080	0.102	–	–	12.66–	12.91–	–	–
	0.007	0.016	–	–	12.90	13.22		
020	0.131	0.174	0.093	0.180	12.46–	12.66–	12.65–	12.78–
	0.024	0.034	0.020	0.038	12.92	13.16	12.99	13.32
021	0.074	0.100	–	–	12.76–	13.24–	–	–
	0.019	0.026	–	–	13.03	13.57		
022	0.092	0.113	–	–	14.60–	14.74–	–	–
	0.089	0.108	–	–	15.15	15.38		
023	0.086	0.106	–	–	12.78–	12.99–	–	–
	0.011	0.013	–	–	13.04	13.30		
024	0.081	0.103	–	–	13.25–	13.50–	–	–
	0.121	0.105	–	–	13.79	14.03		
	–	0.011	–	–				
025	–	–	0.103	0.134	–	–	17.91–	17.95–
	–	–	0.041	0.057			18.39	18.50
026	0.095	0.132	–	–	13.58–	13.73–	–	–
	0.013	0.012	–	–	13.87	14.11		
027	0.078	0.086	–	–	11.22–	11.46–	–	–
	0.019	0.021	–	–	11.48	11.75		
028	0.165	0.184	–	–	15.20–	15.52–	–	–
	0.036	0.044	–	–	15.95	16.25		

**Table 3 (continued)**

MMRP	Semi-ampl.				Mag. range			
	<i>aV</i>	<i>ag</i>	<i>zr</i>	<i>zg</i>	<i>aV</i>	<i>ag</i>	<i>zr</i>	<i>zg</i>
029	0.053	0.068	—	—	13.76—	14.12—	—	—
	0.042	0.044	—	—	14.08	14.50		
030	0.116	0.132	0.090	0.141	14.66—	14.76—	14.84—	14.83—
	0.058	0.069	0.052	0.078	15.18	15.34	15.23	15.32
031	0.126	0.143	—	—	13.86—	14.29—	—	—
	0.030	0.032	—	—	14.29	14.78		
032	0.103	0.128	—	—	13.15—	13.60—	—	—
	0.022	0.015	—	—	13.48	13.97		
033	0.199	0.240	—	—	11.49—	11.69—	—	—
	0.056	0.036	—	—	12.12	12.35		
034	0.098	0.120	0.084	0.119	13.63—	13.78—	13.73—	13.85—
	0.033	0.045	0.029	0.040	14.03	14.25	13.99	14.25
035	0.162	0.203	—	—	14.89—	14.99—	—	—
	0.067	0.076	—	—	15.77	15.86		
036	0.129	0.131	0.120	0.195	13.69—	14.60—	12.70—	14.97—
	0.067	0.064	0.061	0.104	14.15	15.21	13.26	15.66
037	0.073	0.081	0.059	0.086	14.45—	14.90—	14.03—	14.93—
	0.049	0.056	0.041	0.060	14.80	15.35	14.26	15.28
038	0.057	0.071	—	—	14.20—	14.40—	—	—
	0.025	0.032	—	—	14.50	14.72		
039	0.058	0.071	0.042	0.070	14.46—	14.70—	14.21—	14.72—
	0.106	0.130	0.076	0.129	15.00	15.38	14.57	15.24
	>0.014	0.018	0.011	0.015				
040	0.130	0.161	0.117	0.178	14.08—	14.67—	13.59—	14.87—
	0.020	0.025	0.016	0.024	14.54	15.25	13.96	15.37
041	0.094	0.121	0.091	0.153	14.85—	15.35—	14.71—	15.50—
	0.030	0.039	0.027	0.045	15.40	16.00	15.12	16.01
042	0.136	0.161	—	—	11.63—	11.89—	—	—
	0.020	0.026	—	—	12.04	12.34		

**Table 3 (continued)**

MMRP	Semi-ampl.				Mag. range			
	<i>aV</i>	<i>ag</i>	<i>zr</i>	<i>zg</i>	<i>aV</i>	<i>ag</i>	<i>zr</i>	<i>zg</i>
043	—	—	0.127	0.189	—	—	17.26–	19.7–
	—	—	0.117	0.185			18.06	21.0
044	0.080	0.104	—	—	11.49–	11.73–	—	—
	0.018	0.021	—	—	11.73	12.05		
045	0.075	0.088	0.052	0.089	12.47–	12.72–	12.40–	12.73–
	0.022	0.027	0.016	0.029	12.72	13.01	12.59	13.02
046	—	—	0.147	—	—	—	18.16–	20.9–
	—	—	0.022	—			18.64	21.7
047	—	—	0.151	0.233	—	—	17.60–	19.5–
	—	—	0.033	0.058			18.09	20.2
048	—	—	0.135	0.201	—	—	17.80–	19.7–
	—	—	0.031	0.045			18.20	20.4
049	0.042	0.045	0.029	0.047	13.77–	13.90–	13.84–	13.96–
	0.143	0.150	0.109	0.156	14.25	14.41	14.16	14.43
050	—	—	0.162	0.227	15.30–	15.92–	15.35–	16.55–
	—	—	0.040	0.058	15.75	16.45	15.90	17.34

**Table 3a. Semi-amplitudes and magnitude ranges. Known multi-mode variables**

MMRP_J	aV	Semi-ag	ampl zr	zg	aV	Mag. ag	range zr	zg
044322.93+465703.6	0.245 0.047	0.270 0.063	0.185 0.043	0.261 0.062	14.15– 14.89	14.79– 15.72	13.55– 14.08	14.75– 15.58
054223.13+275647.6	0.206 0.024	0.251 0.042	– –	0.240 –	12.48– 13.08	12.89– 13.61	– –	12.99– 13.53
074438.61+291222.8	0.201 0.012	0.224 0.013	– –	0.233 0.013	11.92– 12.42	11.94– 12.53	– –	11.94– 12.50
093044.09+320916.8	0.115 0.186	0.135 0.206	0.112 0.157	0.141 0.213	15.65– 16.70	15.66– 16.75	15.66– 16.30	15.67– 16.53
094051.03+345205.2	0.147 0.178	0.188 0.205	0.125 0.148	0.170 0.202	14.37– 15.32	14.40– 15.42	14.50– 15.15	14.44– 15.34
105408.01–580421.2	0.059 0.074	0.071 0.096	– –	– –	14.24– 14.66	14.52– 15.03	– –	– –
111130.57–632636.4	0.068 0.036	0.088 0.046	– –	– –	12.40– 12.71	12.66– 13.00	– –	– –
143130.85+225023.4	0.063 0.204	0.079 0.239	0.045 0.157	0.067 0.217	15.4– 16.1	15.5– 16.4	15.45– 15.93	15.48– 16.15
151609.22+320007.3	0.152 0.150	0.191 0.216	0.132 0.151	0.193 0.232	15.6– 16.5	15.6– 16.8	15.78– 16.47	15.70– 16.73
160331.49–494754.4	0.058 0.133 –	0.068 0.161 0.013	– – –	– – –	13.43– 13.94	13.86– 14.46	– –	– –
171059.14–351034.8	0.018 0.069	0.019 0.083	– –	– –	13.54– 13.82	14.09– 14.40	– –	– –
185513.28+081813.4	– –	– 0.084	0.190 0.144	0.316	– –	– –	17.43– 18.28	19.6– 21.1
202946.51+374539.5	0.021 0.011	– –	0.179 0.070	0.291 0.107	13.88– 14.05	– –	14.65– 15.31	17.40– 18.42
211839.91+504732.9	0.364 0.022	0.424 0.030	0.276 0.014	0.423 0.023	14.23– 15.25	15.10– 16.29	13.51– 14.19	15.09– 16.09

**Table 4. Color indices and Galactic latitudes. New MMRP-stars**

MMRP	$J - K$ , 2MASS	$B - V$ , APASS	$g' - r'$ , APASS	$g - V$ , ASAS-SN	$g - r$ , ZTF	$b$ , deg
001	0.59	1.22	0.93	—	0.92	+0.5
002	0.59	0.86	0.62	0.53	0.97	-0.7
003	—	—	—	—	0.21	-46.4
004	0.82	1.50	1.30	0.67	1.43	+0.4
005	0.47	0.89	0.71	0.38	—	-3.4
006	0.25	—	—	—	0.33	-12.9
007	0.17	0.33	0.18	0.12	0.17	-13.6
008	0.81	1.47	1.29	0.69	1.42	+3.8
009	0.55	1.14	1.02	0.58	1.01	+0.3
010	0.47	0.91	0.72	0.45	0.82	-2.9
011	0.49	0.83	0.70	0.40	0.74	+0.9
012	0.18	0.34	0.17	0.18	—	-25.1
013	—	—	—	—	0.87	-4.7
014	—	0.41	0.11	—	0.16	+26.8
015	0.23	0.46	0.25	0.19	0.22	+6.7
016	0.25	0.42	0.27	0.17	—	-19.0
017	0.58	0.46	0.20	—	0.37	+5.1
018	0.21	0.50	0.31	0.22	0.28	+8.6
019	0.30	0.67	0.44	0.28	—	-12.2
020	0.26	0.44	0.28	0.22	0.32	+5.0
021	0.92	1.14	1.06	0.51	—	-2.6
022	0.24	0.50	0.32	0.23	—	+9.4
023	0.23	0.52	0.32	0.24	—	+11.0
024	0.28	0.55	0.41	0.24	—	+9.7
025	—	—	—	—	0.08	+51.6
026	0.19	0.45	0.26	0.21	—	+21.8
027	0.29	-0.14 ?	0.47	0.25	—	+3.7
028	0.31	0.67	0.52	0.28	—	+22.8
029	0.58	0.71	0.57	0.38	—	+11.7
030	0.22	0.22	-0.02	0.14	0.05	+30.0
031	0.49	0.91	0.70	0.42	—	-0.5
032	0.59	1.00	0.87	0.47	—	+2.0
033	0.32	0.60	0.54	0.24	—	-3.6
034	0.13	0.39	0.18	0.17	0.22	+9.9
035	—	0.34	-0.01	0.13	—	-19.8
036	1.04	2.39	2.18	1.01	2.36	+1.0
037	0.51	1.07	0.93	0.53	0.99	-1.1
038	0.25	0.49	0.29	0.22	—	-27.0
039	0.41	0.62	0.47	0.30	0.61	+5.3
040	0.57	1.42	1.23	0.67	1.38	+2.9
041	0.43	1.03	0.90	0.62	0.85	+2.4
042	0.28	0.51	0.36	0.32	—	+7.1
043	1.26	—	—	—	2.63	-0.0
044	0.35	0.67	0.42	0.29	—	-4.0

**Table 4 (continued)**

MMRP	$J - K$ , 2MASS	$B - V$ , APASS	$g' - r'$ , APASS	$g - V$ , ASAS-SN	$g - r$ , ZTF	$b$ , deg
045	0.25	0.75	0.54	0.28	0.38	-0.5
046	1.35	-	-	-	2.85	-1.0
047	1.05	-	-	-	1.95	+4.3
048	1.07	-	-	-	2.04	+2.5
049	0.23	0.45	0.20	0.15	0.22	-12.7
050	0.73	-	1.52	0.67	1.36	+2.3

**Table 4a. Color indices, and Galactic latitude. Known multi-mode variables**

MMRP	$J - K$ , 2MASS	$B - V$ , APASS	$g' - r'$ , APASS	$g - V$ , ASAS-SN	$g - r$ , ZTF	$b$ , deg
044322.93+465703.6	0.81	1.58	1.42	0.70	1.37	+0.6
054223.13+275647.6	0.58	1.06	0.89	0.48	-	-1.1
074438.61+291222.8	0.20	0.27	0.06	0.09	-	+23.7
093044.09+320916.8	0.12	0.18	0.00	0.17	0.16	+46.5
094051.03+345205.2	0.26	0.20	0.19	0.11	0.11	+48.8
105408.01-580421.2	0.37	0.72	0.57	0.32	-	+1.3
111130.57-632636.4	0.44	0.69	0.55	0.31	-	-2.7
143130.85+225023.4	0.23	0.46	0.15	0.20	0.14	+67.0
151609.22+320007.3	0.19	0.17	0.03	0.15	0.13	+58.3
160331.49-494754.4	0.59	0.84	0.72	0.48	-	+2.1
171059.14-351034.8	0.53	1.13	1.06	0.57	-	+2.6
185513.28+081813.4	1.19	-	-	-	2.48	+2.9
202946.51+374539.5	1.41	-	-	-	2.99	-0.8
211839.91+504732.9	1.07	1.90	1.73	0.92	1.86	+0.9